doi:10.1111/evo.14647

SSE Society for the Study of Evolution

EVOLUTION INTERNATIONAL JOURNAL OF ORGANIC EVOLUTION

Evolutionary loss of shell pigmentation, pattern, and eye structure in deep-sea snails in the dysphotic zone

Suzanne T. Williams,[1,2] Emily S. Noone,[1,3] Lisa Marie Smith,[1,4] and Lauren Sumner-Rooney[5]

[1]*Department of Life Sciences, Natural History Museum, London SW7 5BD, United Kingdom*

[2]*E-mail: s.williams@nhm.ac.uk*

[3]*Department of Life Sciences, Imperial College, London SL5 7PY, United Kingdom*

[4]*Current Address: National Institute of Water and Atmospheric Research, Wellington 6021, New Zealand*

[5]*Museum für Naturkunde, Leibniz Institute for Biodiversity and Evolution DE-10115, Berlin, Germany*

Received February 1, 2022

Accepted September 26, 2022

Adaptations to habitats lacking light, such as the reduction or loss of eyes and pigmentation, have fascinated biologists for centuries, yet have rarely been studied in the deep sea, the earth's oldest and largest light-limited habitat. Here, we investigate the evolutionary loss of shell pigmentation, pattern, and eye structure across a family of deep-sea gastropods (Solariellidae). We show that within our phylogenetic framework, loss of these traits evolves without reversal, at different rates (faster for shell traits than eye structure), and over different depth ranges. Using a Bayesian approach, we find support for correlated evolution of trait loss with increasing depth within the dysphotic region. A transition to trait loss occurs for pattern and eye structure at 400–500 m and for pigmentation at 600–700 m. We also show that one of the sighted, shallow-water species, *Ilanga navakaensis*, which may represent the "best-case" scenario for vision for the family, likely has poor spatial acuity and contrast sensitivity. We therefore propose that pigmentation and pattern are not used for intraspecific communication but are important for camouflage from visual predators, and that the low-resolution vision of solariellids is likely to require high light intensity for basic visual tasks, such as detecting predators.

KEY WORDS: Deep sea, evolution of trait loss, gastropod, pattern, pigment, vision.

Evolution in dark habitats, such as the deep sea, caves, underground, or within other organisms, often produces phenotypes that reflect the absence or scarcity of light, including changes to appearance, sensory biology, and biological rhythms. Of all these dark habitats, the deep sea is the largest and oldest on the planet, and has arguably the greatest scope for evolutionary studies. It offers an abundance of different habitats and lifestyles, long timescales for migration and radiation, gradients of light intensity and spectral availability, and widespread bioluminescence. Moreover, the reduction and loss of visual traits (such as pigmentation, pattern, and vision) in the deep sea occurs in a wide range of species, across habitats, trophic levels, and phylogenetic groups (e.g., Munk 1965; Warrant and Locket 2004; Johnsen 2005; Syme and Oakley 2012; Williams et al. 2013; Sumner-Rooney et al. 2016; Gonzalez et al. 2017). This diversity provides the opportunity to disentangle which factors contribute to the evolution of visual traits in the dark, and to examine the evolutionary dynamics of how, where, and when trait loss occurs.

Much of the focus to date in the marine realm has been on pelagic taxa, and there is scant information about how pigmentation and vision co-evolve in slow-moving or sessile benthic deep-sea invertebrates, which are ecologically critical. Benthic taxa are particularly useful for studying the loss of visual traits. They are more likely to live a sedentary lifestyle, have tactile or chemosensory cues available to them, may rely less on visual cues in shallow water, and remain at a relatively constant depth. These characteristics may not only predispose them to the loss

of visual traits with increasing depth (Sumner-Rooney 2018), but also make it easier to characterize relationships between habitat depth and trait loss.

The gastropod family Solariellidae is an emergent model system for studying the evolution of trait loss in deep sea benthic organisms. It spans enormously diverse oceanic habitats, ranging from the intertidal to the abyss (>4,000 m; Bagirov 1995), and its highest species diversity is found on the outer shelf and continental slope (100−1,000 m) (Williams et al. 2020), where evolutionary transitions driven by diminishing sunlight are most likely to occur. Solariellid lineages have undertaken multiple habitat shifts into deeper water (Williams et al. 2013) and eye loss has evolved in at least seven independent events (Williams et al. 2013; Sumner-Rooney et al. 2016), via variable morphological pathways (Sumner-Rooney et al. 2016). Although these studies suggested eye loss was related to shifts into deep water, this was not explicitly tested. Pigmentation and pattern, which are widespread in shallow-water species, have not been studied in the context of depth, and nothing is known about solariellid visual ability or ecology to date.

To address these gaps, and further develop solariellids as a model for evolution in the deep sea, we investigated the occurrence of three visual traits: eyes, shell pigmentation, and shell pattern, in correlation with habitat depth. Beyond confirming that changes to eye structure, pigmentation, and pattern are associated with increasing depth, we also aimed to characterize how such changes take place. Namely, does the evolution of loss occur along a continuous gradient, or at threshold depths? At what depths do losses occur? What can the speed, location, and order of these changes tell us about the factors influencing their evolution, and their relationship to one another? We specifically test to see if trait loss is correlated with depth across its full range (from intertidal to abyssal) or is dependent on threshold light intensities. In the latter case, within shallow depths, above some light intensity threshold, we might expect no correlation between depth and trait presence/absence. Equally, in depths below the light intensity threshold, there will again be no correlation of visual traits with depth. A correlation would only be expected over an area where the changing light intensity affects trait presence/absence, with the exact width and location of the transition zone varying by trait. Across the full depth range, the correlation between trait and depth is weakened by the presence of noise in shallow and deep depths where traits do not change. Conversely, by dividing the data into two depth categories and iteratively adjusting the boundary value, we can pinpoint the location of the transition zone by comparing trait presence/absence between depth categories. If traits are independent of depth, there should be no correlation in any analysis. As visual traits in solariellids are poorly understood, we also conducted preliminary investigations into the basic nature of pigmentation and estimate the visual acuity and sensitivity in a single shallow-water species.

Materials and Methods

TRAIT DATA

Trait data were recorded from samples used in the molecular phylogeny, of which the majority were collected by the Muséum national d'Histoire naturelle (MNHN) within the last two decades and preserved in ethanol. Some additional MNHN specimens, including formalin-preserved and dry specimens, and material from other museums were also included. Shell color and pigment in solariellids are robust to different types of preservation and eye characters can be recorded from both ethanol and formalin-preserved specimens. See Figure 1 for examples of each trait, Table S1 for list of specimens used and GenBank Accession Numbers, and Table S2 for trait data.

Solariellids have small, nacreous shells that may be colored, predominantly with yellow, reddish-brown, or brown pigments, often with species-specific color patterns, or lacking in pigmentation. Shell pigmentation was recorded as present (1) for pigmented shells (outer layer only) or absent (0) for species with white, cream, buff, off-white, or pale gray shells, with or without iridescence. We did not score shell iridescence associated with nacre, as this is not conferred by pigmentation. Where a species showed intraspecific variation, pigmentation was scored as present. Pigmentation was recorded for the outermost layer of the shell, even if this was partially corroded.

As nothing is known about shell pigments in solariellids, we also conducted preliminary investigations into the basic nature of pigmentation to establish whether shell pigment (and thus, the basis for pattern) was likely to be of dietary origin or synthesized de novo, as only the latter can be directly heritable and therefore subject to selection. Shells from 12 species representing different genera across the complete range of depths where pigmented specimens are found were examined under UV light to see whether they exhibited any fluorescence (see Table S3 for list of species examined and their depths). Such fluorescence is likely of no biological significance to the animals, but is a useful first step to the chemical identification of pigments (e.g., Williams et al. 2016), which in turn is useful for determining whether shell color is likely to be heritable (Williams 2017).

Shell pattern was scored as present (1) for spots, flames, wavy lines, reticulating networks (e.g., Fig. 1c), zig-zags, or prosocline variations in color intensity (e.g., Fig. 1b), or absent (0) for uniform coloration or irregular washes of color. Where the upper surface of the body whorl was uniformly pigmented but the lower half or the base of the shell was unpigmented (Fig. 1f), shells were scored as lacking pattern. To be scored as "patterned," markings needed to be approximately consistent in location and

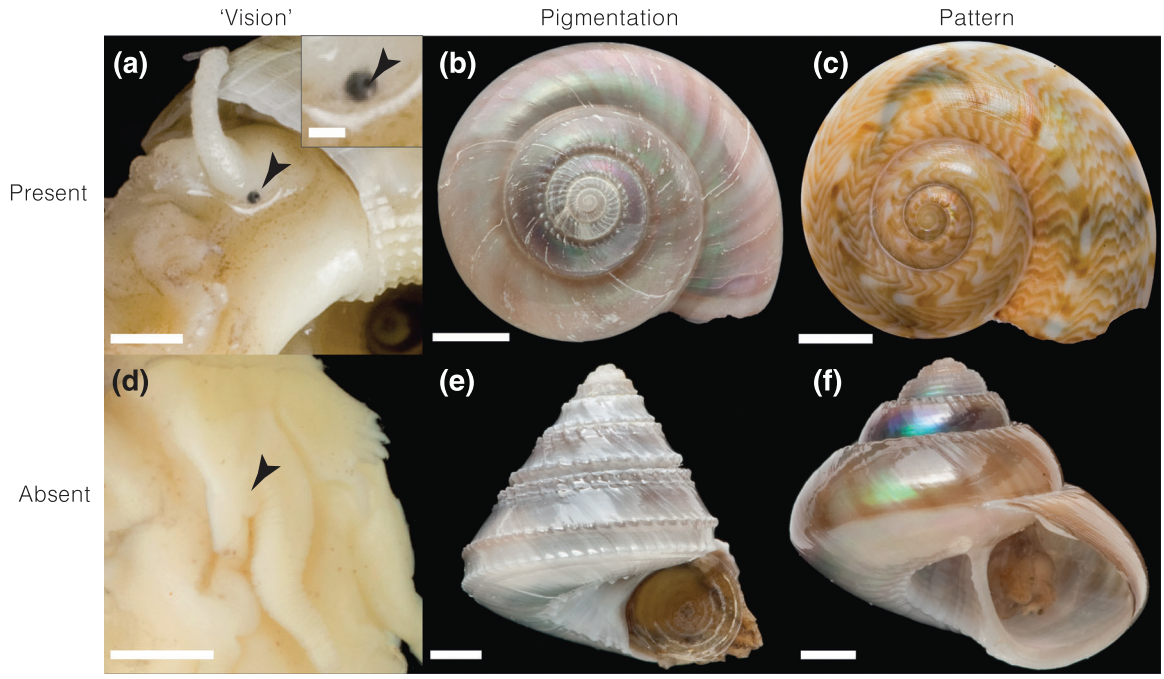

Figure 1. Solariellid exemplar species illustrating different morphological traits. Shells are oriented to best illustrate trait. (a) Species with presumed functional eye (indicated with arrow) having both black pigment and open aperture. *Spectamen* sp. 1, MNHN IM-2007-18351, scale bar: 500 μm. Inset: Detail of eye; arrow indicates open aperture. Scale bar: 100 μm. (b) Shell with pigmentation and pattern of prosocline radiating bands of different pigment density. *Elaphriella cantharos*, MNHN IM-2009-15185, scale bar: 3 mm. (c) Shell with pigmentation and complex, reticulate pattern. *Ilanga gotoi*, MNHN IM-2007-18349, scale bar: 3 mm. (d) Blind species. Arrow indicates eye stalk. *Bathymophila* sp. 27, MNHN IM-2013-59009, scale bar: 500 μm. (e) Shell lacking pigmentation. *Arxellia tenorioi*, MNHN IM-2007-18425, scale bar: 2 mm. (f) Shell with pigmentation but no pattern. *Archiminolia* sp. 1, MNHN IM-2007-18540, scale bar: 1 mm. All photos © NHM.

form among a subset of specimens, where multiple specimens were available, as evidence that the observed pattern is heritable. Where species were represented by a single specimen, it was assumed to be representative.

Eye morphology was examined using a dissecting microscope. Solariellid eyes are of the "open cup" type, lacking a cornea and with an open aperture to the vitreous body (Sasaki 1998). Eyes (hereafter referred to as "vision," with the caveat that we lack functional data) were scored as present (1) when black retinal pigment and a visible aperture were observed in the eye (e.g., Fig. 1a). Where either was lacking, eyes were scored as (0) (e.g., Fig. 1d). Visual status of most species was based on a previous study using the same criteria (Sumner-Rooney et al. 2016), and new data were added for 28 species examined for this study. These include the first data for the genus *Lamellitrochus*, which was not included in previous studies, and additional species from 12 genera.

The minimum depth (hereafter, "depth") at which a species is known to occur was recorded from literature and/or our own unpublished data (see Table S2). Minimum depth was chosen as the most conservative proxy for light availability, as it represents the area of a species range where light is most likely to be present and eyes, pigment, and pattern are likely to be of selective value. Where literature records were used, they were based on live-collected specimens only, as dead shells may be found in significantly deeper water (Quinn 1979). For undescribed species, or where species boundaries or identifications remain uncertain, data were based only on specimens used in molecular studies.

SEQUENCE DATA AND ALIGNMENT

DNA was extracted from 28 solariellid species, and gene fragments for 28S rRNA (28S), 12S rRNA (12S), 16S rRNA (16S), and cytochrome oxidase I (COI) were amplified and sequenced following Williams and Ozawa (2006). Combined with previously published sequences (Williams et al. 2008, 2013; Sumner-Rooney et al. 2016; Vilvens and Williams 2020), this produced a dataset of 92 solariellid species having both sequence data and complete morphological data (Table S1). Ribosomal RNA (rRNA) sequences were aligned in PASTA (version 1.8.5; Mirarab et al. 2014) using the following options: MAFFT (Katoh et al. 2009) to align, OPAL (Wheeler and Kececioglu 2007) to merge, FASTTREE (Price et al. 2009) to estimate, GTR+G20 as the nucleotide substitution model, 50% subproblem and MinCluster decomposition with five iterations, and the best alignment

determined by likelihood value. GBLOCKS (Castresana 2000) was used to remove ambiguously aligned regions from rRNA alignments (four-gene alignment is in Supplementary Data S4).

PHYLOGENETIC ANALYSIS OF SEQUENCES AND TRAITS AND SIMULTANEOUS ANCESTRAL STATE RECONSTRUCTIONS

We analyzed trait data using a Bayesian approach in BEAST (version 1.10.4; Drummond and Rambaut 2007), while simultaneously reconstructing a time-calibrated phylogenetic framework. The concatenated four-gene dataset was analyzed with depth, pigmentation, pattern, and "vision" data, with an uncorrelated relaxed clock with lognormal distribution for molecular data and a strict clock for trait data, and a Yule speciation model. Trees for each partition were linked, but substitution models and clock rates were free to vary. Nucleotide substitution models were determined using MODELTEST-NG (Darriba et al. 2020) (HKY+I+G for 12S and GTR+G+I for other genes). The tree was calibrated using fossil dates for three taxon groups. *Solariella* sp. from the latest Oligocene of the Lincoln Creek Formation in western Washington State, USA (Kiel 2010) was used to date the genus *Solariella*. *Zetela awamoana* Laws 1939, from the later half of the Burdigalian (early Miocene) of the Mount Harris Formation, South Island, New Zealand (Beu 1990) was used to calibrate *Zetela* (for details, see Williams et al. 2013). "*Solariella*" *montsecana* from the Campanian of Torallola, Spain (Kiel and Bandel 2001) was used to calibrate the ingroup. "*Solariella*" *montsecana* is similar to "*Solariella*" *mexcalensis* from lower Maastrichtian of the Mexacala Formation in Mexico (Kiel et al. 2002) and both are very similar to *Arxellia*, but Williams et al. (2013) noted that "*S*." *montsecana* has axial ribs in the umbilicus and so likely represents a different genus. Equally, "*S*." *mexcalensis* appears to have beading inside the umbilicus, which is not found in *Arxellia* (Vilvens et al. 2014; Williams et al. 2020). Priors were set using a lognormal distribution: tmrca(all solariellid samples): 95% quantiles: 72.38−107.2 Myr (mean in real space [MIR]: 10, SD: 10: offset 71), starting age 75 Myr; tmrca(*Solariella*): 95% quantiles: 23.62−34.38 Myr (MIR: 3.5, SD: 3; offset: 23), starting age 25 Myr; and tmrca(*Zetela*): 95% quantiles: 16.67−27.97 Myr (MIR: 2.5; SD: 3.65; offset: 16.5), starting age 20 Myr. The analysis ran for 60,000,000 generations sampling every 3,000 generations until effective sample sizes (ESS) values were greater than 200 for all parameters (determined using TRACER) (Rambaut et al. 2018). A maximum clade credibility tree with median node heights was produced using TREEANNOTATOR (version 1.10.4; Drummond and Rambaut 2007) from 18,000 trees after 10% burn-in.

We inferred a continuous phylogeographic diffusion model for the depth at which each species was found using a Brownian random-walk model (Gill et al. 2017). Pigmentation, pattern, and "vision" were analyzed using an asymmetric substitution model, which specifies a discrete phylogeographic analysis using nonsymmetric rates between states. We used a Bayesian stochastic search variable selection (BSSVS) model to test for significance of rate changes between trait states using Bayes Factors (Lemey et al. 2009). Bayes Factors were calculated from BSSVS log files using SPREAD3 version 0.9.7.1 (Bielejec et al. 2011). We also ran an independent analysis without BBSVS to report rate changes. Ancestral state reconstructions were performed for all traits and state change counts were reconstructed for morphological traits using Markov Jumps (Minin et al. 2008).

TESTING FOR PHYLOGENETIC SIGNAL

We tested for phylogenetic signal for morphological traits using *D* (Fritz and Purvis 2010), implemented by the function *phylo.d* in the R package "Caper" (Orme et al. 2012), and for five indices (Moran's *I* [Moran 1948, 1950], Abouheif's C_{mean} [Abouheif 1999], Blomberg's *K* and *K** [Blomberg et al. 2003], and Pagel's λ [Pagel 1999]) for $\log_{10}$-transformed depth data using the R package "phylosignal" (Keck et al. 2016). We also calculated Local Indicators of Phylogenetic Association (LIPA) using Local Moran's *I* (*Ii*) with the R function *lipaMoran* in "phylosignal" for each tip of the phylogeny for $\log_{10}$-transformed depth data.

RELATIONSHIPS WITH DEPTH

To visualize depth distribution, depth ranges were plotted for each genus based on depths of all species used in the molecular tree, plus 22 additional species. These additional species were missing morphological data and so were not included in phylogenetic or correlation studies but have depth data and molecular data to confirm phylogenetic assignment to genus or clade. One-way ANOVA and Tukey's range test were used to determine significant differences in depth distribution among genera.

We used both continuous and binarized depth data to test for correlation with loss of eye function, shell pigmentation, and pattern in samples collected from 0−1185 m. We used binarized data in BAYESTRAITS (version 3.0.2) (Pagel and Meade 2007) to explore the nature and location of evolutionary transitions, focusing on the dysphotic zone, where most evolutionary transitions have been recorded in other taxa and where we have the greatest number of species. Depth data were binarized into "shallow" and "deep" categories to effectively test whether trait presence or absence was more common in one or other of these. The "shallow" category was initially defined as <200 m and "deep" as ≥200 m. We then separately analyzed the same data using a series of eight different cutoff values at 100 m intervals across the dysphotic zone (200−900 m). For each dataset, we determined whether the trait value and depth category are linked (dependent model) or unlinked (independent model). By iteratively adjusting the cutoff value, we attempted to pinpoint shifts between the two models.

The analysis was based on a sample of 500 BEAST trees taken from the BSSVS analyses to allow for phylogenetic uncertainty. Three independent analyses were performed for each cutoff value using Markov Chain Monte Carlo (MCMC) and "Discrete" options. Marginal likelihood was calculated using a stepping-stone sampler with 1,000 stones, and 10,000 iterations for pigmentation and pattern and 5,000 stones with 20,000 iterations for "vision," which showed variation between repeat analyses in preliminary runs. Support was determined using Bayes Factors following Rafferty in Gilks (1996, pp. 163−188), comparing the average marginal likelihood for the three runs for a dependent model and an independent model using: Log BF = 2(log marginal likelihood dependent model – log marginal likelihood independent model).

We also evaluated morphological traits as phylogenetically nonindependent variables of log-transformed, continuous depth data using the function *brunch* in the R package "Caper" (version 0.5.2; Purvis and Rambaut 1995; Orme et al. 2013), to test whether loss evolves along continuous depth gradients, as opposed to below threshold depths. "*Brunch*" estimates phylogenetically independent contrast values of a continuous trait on the nodes where each side can be unequivocally attributed to one or other of the trait categories. Significance was determined using a one-tailed *t*-test and *F*-statistic. We also tested for evolutionary covariation using the *threshBayes* function in "phytools" (Revell 2012). *threshBayes* uses Bayesian Inference to test for evolutionary covariation between continuous and discrete traits by looking for a correlation in liabilities. We ran MCMC analyses for 2.5 million generations, with a sampling interval of 1,000 and a burn-in of 10% prior to summarizing posterior distribution values for the correlation coefficient I. We determined significance by assessing ESS of the correlation coefficient using *effectiveSize* and Highest Posterior Density (HPD) interval using *HPDinterval* in the R package "coda" (Plummer et al. 2006).

ESTIMATION OF VISUAL PARAMETERS IN *Ilanga navakaensis* (LADD, 1982)

To provide context for the interpretation of eye and pattern loss, we collected preliminary data relating to visual ability from histological sections of *Ilanga navakaensis*. This species was chosen because it has a large eye size compared to other solariellids, tropical distribution, and shallow depth range. As such, this species could provide a "best estimate" of visual ability and its relative importance under the most amenable light conditions, giving a tentative indication as to whether acuity is likely to be sufficient to detect shell pattern in conspecifics, and whether sensitivity could be sufficient to support transitions to deeper water. However, these estimates are based solely on morphology in a single individual; they are intended only to give an idea of feasible visual function and should not be interpreted as true functional data.

To estimate optical sensitivity, photoreceptor diameter and length were measured from existing histological sections from a single individual (as *Ilanga* 6; Sumner-Rooney et al. 2016). Focal length was estimated from three-dimensional models of two eyes from the same individual, one produced from histological sections (Sumner-Rooney et al. 2016) and one by micro-CT (Sumner-Rooney et al. 2019). A digital section was cut through the central axis of the eye and estimated focal length was measured at 46 equally spaced points around the retinal cup. In the absence of data on its optical properties, focal length was estimated from the centroid of the vitreous body to the distal tips of the photoreceptors. We used this conservative estimate as it is likely that the vitreous body has only weak focusing power. Optical sensitivity was calculated using the Land equation (Land 1981), for both shallow-water (broad-spectrum light) and deep-water (monochromatic light) habitats to explore the effect of habitat shifts, with the photoreceptor absorption coefficient, *k*, defined as 0.0067 μm^{-1} (Warrant and Nilsson 1998).

To estimate "best case" spatial resolution (i.e., limited only by interreceptor angle), we measured the angle subtended by adjacent photoreceptors and the centroid of the vitreous body. We then used this value and the R package "AcuityView" (Caves and Johnsen 2017) to transform images of an *I. navakaensis* shell and of a living solariellid, *Ilanga laevissima*, against its natural substrate. As the field of view is not known for *I. navakaensis*, we cannot be sure of the viewing distance at which these images would fill the field of view at their true size. We therefore used viewing distances of 1, 3, and 5 cm for comparison. Vision was assumed to be monochromatic, as there is no evidence of color vision in gastropods, and to provide a "best case" scenario for resolution.

Results

TRAIT OBSERVATIONS

Three morphological traits were recorded: presence of eyes with black pigment and an open aperture, shell pigment, and shell pattern. All new *Bathymophila* species examined lack observable eyes (see Fig. 1d for an example), but other new species exhibited black retinal pigment and open apertures (e.g., Fig. 1a). Assignment of shell pigmentation was straightforward for all but *Bathymophila* sp. 16, which had a yellowish iridescent shell. Comparison with *Bathymophila* sp. 15, which also had a yellow nacreous shell layer and a partially corroded white chalky shell layer on top, suggests that the yellow shell in *Bathymophila* sp. 16 may also be nacreous shell layer exposed by complete corrosion of the overlying layer of shell, but in the absence of that layer, the yellow coloration was conservatively scored as pigmentation occurring on the outer shell layer (Table S2). Intraspecific variation in shell

pigmentation and pattern was found in *Archiminolia* sp. 2, *Elaphriella paulinae* Vilvens and Williams, 2016, *Ilanga harrytaylori* Vilvens and Williams 2020, *Phragmomphalina vilvensi*, *Phragmomphalina* sp. 1, *Microgaza* sp. 1, "*Solariella*" *carvalhoi*. See Table S2 for details and Figure 1 for examples of all traits. All shells examined under UV light exhibited weak-moderate red fluorescence.

PHYLOGENETIC ANALYSES

Examination of morphological traits within a phylogenetic framework suggests that changes between states in shell pigmentation (median 18, 95% HPD: 15−28) and pattern (median 19, 95% HPD: 16−27) occurred more frequently across the tree than changes to "vision" (median 8, 95% HPD: 7−9). Clock rates showed that pattern and pigmentation change about 2.5 times faster than "vision" (4.55×10^{-3}, 4.53×10^{-3}, and 1.84×10^{-3}, respectively). Bayes Factors show that rates from the BSVSS BEAST run for loss of "vision," shell pigmentation, and pattern are all significantly different from zero (BF >> 50), whereas rates of gain are not (BF < 0.5) (see also non-BSSVS analyses; Table S5). All three traits have been lost at different times, and across a larger time range for pattern and pigmentation (Paleocene-Pliocene) than "vision" (Early Eocene-Late Miocene). Ancestral states for key nodes are given in Figure 2.

TESTING FOR PHYLOGENETIC SIGNAL

Testing traits for phylogenetic signal (i.e., "the tendency for related species to resemble each other, more than they resemble species drawn at random from a phylogenetic tree"; Münkemüller et al. 2012), we determined that shell pigmentation had a positive D score ($D = 0.087$, $P_1 < 0.0001$, $P_0 = 0.370$; $n_1 = 59$, $n_0 = 33$), whereas pattern ($D = -0.013$, $P_1 < 0.0001$, $P_0 = 0.523$; $n_1 = 50$, $n_0 = 42$) and "vision" ($D = -0.376$, $P_1 < 0.0001$, $P_0 = 0.902$; $n_1 = 68$, $n_0 = 24$) had negative results. P_1 is the probability of the estimated D arising from no (= random) phylogenetic structure (i.e., $D > 1$) and P_0 is the probability of the estimated D resulting from Brownian phylogenetic structure (i.e., $D \neq 0$). All results were significant for P_1 but not P_0, suggesting that traits were not randomly distributed across the tree but approximately as expected under a Brownian motion model of evolution. The strongly negative value for "vision" suggests more clumping than would be expected under a Brownian model. Log_{10}-transformed depth data also showed significant phylogenetic signal ($P \leq 0.004$) for all five indices tested (C_{mean}: 0.264, I: 0.058, K: 0.546, K*: 0.535, λ: 0.098), with significant autocorrelation observed between phylogeny and depth in deep-water *Bathymophila* and *Zetela* and shallow-water *Ilanga* and *Minolia* in the LIPA analysis (Fig. S1).

RELATIONSHIPS WITH DEPTH

Depth distribution was plotted by genus, for all currently accepted solariellid genera. Our results showed *Minolia*, *Microgaza*, *Ilanga*, *Solariella*, and *Spectamen* are most common in shallow water (median: <200 m), whereas *Bathymophila*, *Chonospeira*, *Zetela*, and Clade D are more common in deeper water (median: >600 m; Fig. 3). One-way ANOVA suggested that genera are distributed at different depths ($F = 6.38$, df = 18, $P < 0.001$; adjusted $R^2 = 0.461$; excluding singletons: $F = 7.20$, df = 15, $P < 0.001$; adjusted $R^2 = 0.458$; Fig. 3). Eyes can be found across the full depth range sampled here ("*Solariella*" *carvalhoi*, 0 m; *Zetela kopua*, 1185 m) (Table S2; Fig. 3). Pigment and pattern are found in species with minimum depth ranges ≤973 m, although this may be an overestimate, as the deepest species, *Spectamen* sp. 4, is known from only two specimens from the same location and other species of this genus are found in much shallower water (see outlier for *Spectamen* in Fig. 3). Excluding this one species, pigment and pattern are found in species with minimum depth ranges ≤692 m.

Analysis of depth data using binarized categories with BayesTraits suggested noncorrelation between pigmentation and depth category when categories were divided at 200 m, but supported a relationship between depth category and pigmentation when categories were divided between 300−900 m, reaching maximum support at cutoffs of 600−700 m. Shell pattern likewise showed no correlation with depth category at cutoffs of 200, 300, 800, or 900 m, with support for correlation with cutoffs from 400−700 m, reaching maximal support at 400−500 m. "Vision" showed a similar pattern, with strong support for noncorrelation at shallow and deeper parts of the dysphotic zone, and weak evidence of correlation with depth category when "shallow" and "deep" categories were divided at 500 m (Fig. 4; Table S6).

Conversely, analysis of depth data as a continuous character revealed little evidence of a correlation with traits. Our results suggest that morphological trait data fit the assumption of Brownian evolution, although the correlation between depth and pattern was only marginally nonsignificant when using log_{10}-transformed depth data with *brunch* (pigmentation: $R^2 = 0.023$, adjusted $R^2 = -0.042$, $F = 0.35$, df = 15, $P = 0.56$, t-value = −0.59; pattern: $R^2 = 0.205$, adjusted $R^2 = 0.155$, $F = 4.13$, df = 16, $p = 0.06$, t-value = −2.032; vision: $R^2 = 0.234$, adjusted $R^2 = 0.124$, $F = 2.14$, df = 7, $P = 0.19$, t-value = −1.461). Testing using *threshBayes*, evolutionary covariation was strongest for "vision" ($r = -0.438$, HPD: −0.813, 8.051×10^{-5}), then pattern ($r = -0.285$, HPD: −0.612, 0.054) and pigmentation ($r = -0.141$, HPD: −0.484, 0.184); however, these results were not significantly different from zero as all HPD ranges span zero, although only marginally for vision. Stationarity was reached within the burn-in phase and ESS values were >200, confirming mixing of the Markov chain.

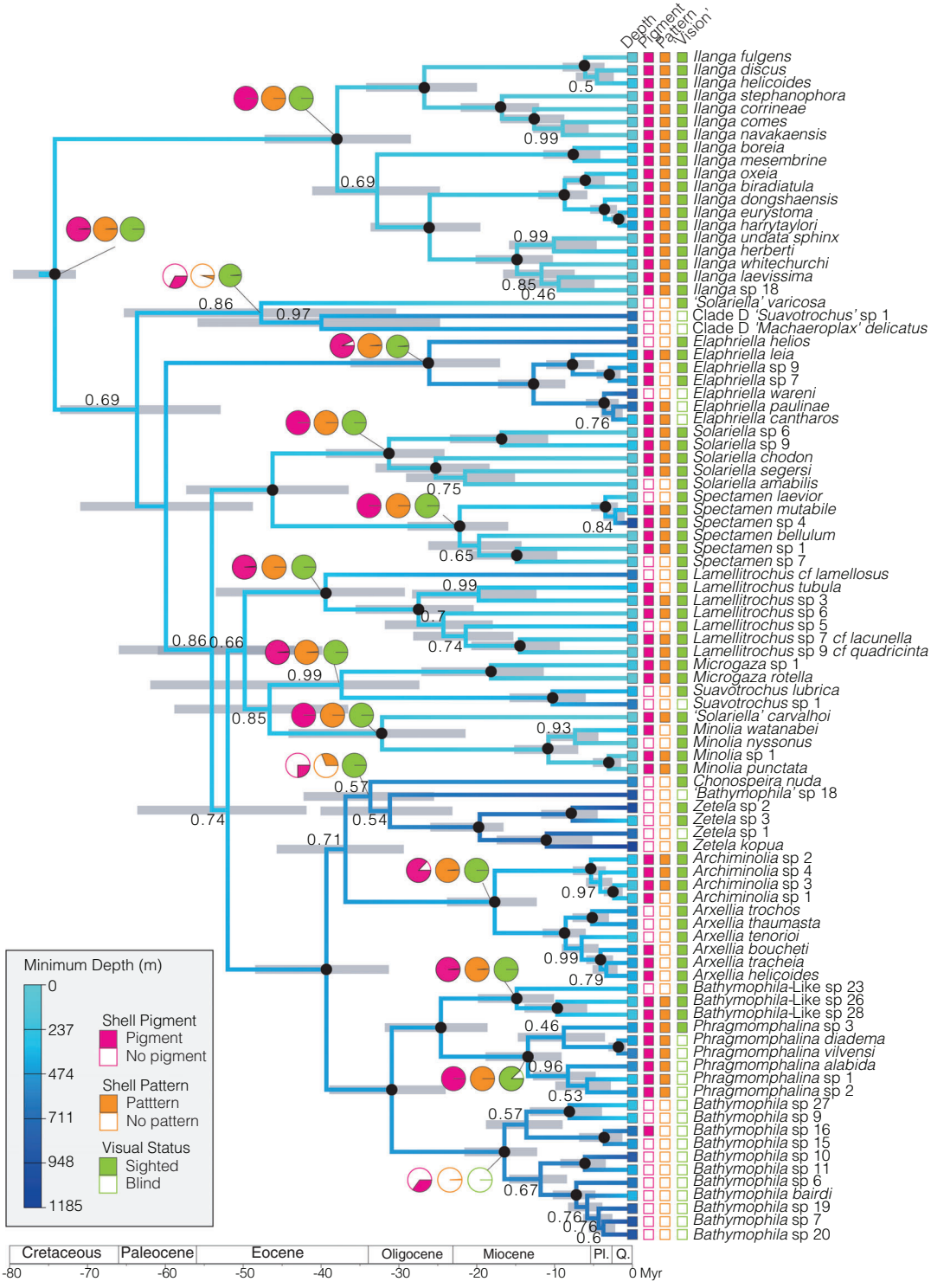

Figure 2. Bayesian analysis of 92 solariellid species representing all known genera as implemented in BEAST (BSSVS analysis). A total of 302 unique clades were found in the 18,000 trees used to calculate the maximum clade credibility tree and the Highest Log Clade Credibility was −11.658. Nodes with maximal support, posterior probability (PP) = 1.0, are indicated by black dots; numbers on branches are PP < 1.0. Root position was determined by BEAST analysis. Minimum depth (m), shell pigmentation, shell pattern, and 'vision' are indicated for each species at tips by box color. Gray rectangles at nodes are 95% highest posterior density intervals for node ages. Pie diagrams indicating ancestral state reconstructions for the three morphological traits are shown for selected clades. Pie slices correspond to PP support for each character state; colors are the same as tip boxes. Ancestral state reconstruction for depth is indicated by branch color: lighter colors represent shallower depths and darker colors are deeper (see Key). Geological epochs: Pl. Pliocene; Q. Quaternary.

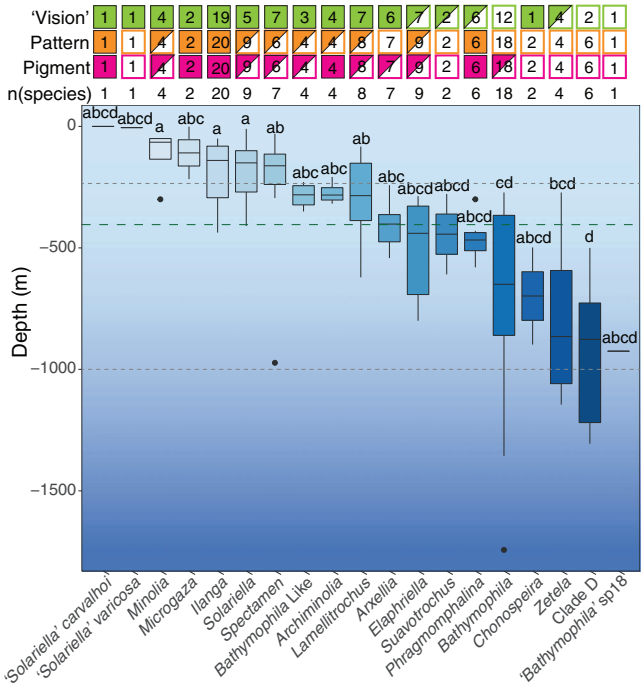

Figure 3. Boxplot showing range of minimum depths for solariellid species used in molecular phylogenetic studies, grouped by genera, and three species not yet assigned to genera. Only species for which molecular data are available to confirm phylogenetic placement have been included. The upper and lower bounds of the box are the 25th and 75th percentiles, horizontal bars represent the median, vertical bars are the largest, or smallest values within 1.5 times the interquartile range, and outliers (>1.5 times or <3 times the interquartile range beyond either end of the box) are shown as circles. Letters indicate significant groups in Tukey analyses, which takes sample size into account. Lightly dotted lines indicate the boundary of the dysphotic zone. The green dashed line marks the average minimum depth for all species. "Vision," shell pigmentation, and shell pattern are indicated for each genus by box color and pattern. Full color: all species have trait. Half square: at least one species has trait. Empty square: trait absent in species sampled. Number in boxes: number of species with data for each trait; n(species): number of species used to plot depth data

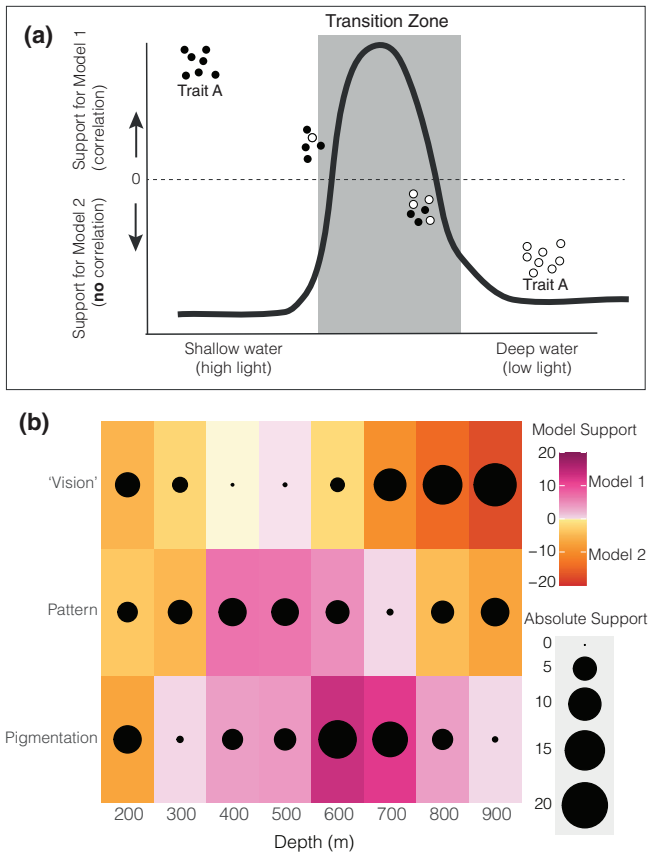

Figure 4. (a) Hypothesized model of correlation between a hypothetical, binary, light-dependent trait (Trait A) and depth. At shallow depths, until light becomes too dim, no correlation will be observed between depth and Trait A. Equally, once light levels become too low, there will again be no correlation with depth. A correlation would only be expected over a transition zone, with the exact width and location of the transition zone varying by trait. (b) Graphical illustration of support for tests for correlated evolution between discrete traits (shell pigmentation, shell pattern, and "vision") and depth (m) for solariellid gastropods based on analysis with BayesTraits. Depth was treated as a binary character and the *x*-axis shows cutoff values for binning depths for eight independent tests. Support is based on Bayes Factor (BF) produced by testing two alternate models (Model 1: dependent/correlated evolution versus Model 2: independent/noncorrelated evolution) in BayesTraits. The larger (more positive) the BF value, the greater the support for correlated evolution, and the smaller (more negative) the BF, the greater the support for Model 2 (no correlation). The size of the dot shows the absolute value of BF, and color and intensity of the tile show scale of support, with darker colors indicating stronger support: pink tiles are positive, showing support for Model 1; orange tiles are negative results showing support for Model 2. As we predicted, there is a clear shift between Model 2 (trait is not correlated with depth) and Model 1 (trait is correlated with depth) for characters across the dysphotic zone.

ESTIMATION OF VISUAL PARAMETERS IN *Ilanga navakaensis*

Investigating visual acuity for a shallow-water solariellid with (comparatively) large eyes, we found that mean photoreceptor diameter (and thus, in this contiguous retina, photoreceptor separation) was 4.5 μm (SD = 0.78 μm, $n = 80$) and mean projection length was 28.8 μm (SD = 9.91 μm, $n = 80$). Mean estimated focal length was 56.4 μm (SD = 17 μm, $n = 46$), giving a mean interreceptor angle of 4.3°. Optical sensitivity was calculated to be 0.44 in shallow water, and 1.0 in deep water. With the best possible resolution of 4.3°, at a viewing distance of 1 cm, the overall shape of a conspecific shell and a living solariellid against natu-

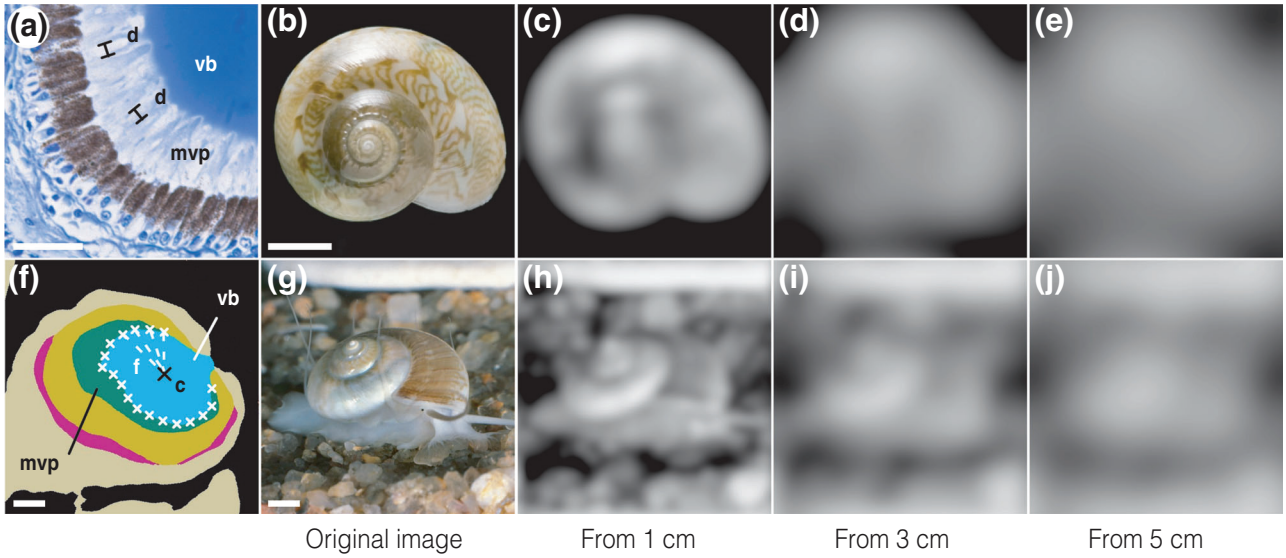

Figure 5. Estimated "best-case" visual acuity in a shallow-water solariellid, *Ilanga navakaensis*. (a) Diameters ("d") of photoreceptor microvillar projections ("mvp") were measured from histological sections taken by Sumner-Rooney et al. (2016). (b) A patterned, pigmented *Ilanga navakaensis* shell. (c–e) View of shell in (b) transformed through the estimated best-case acuity for *I. navakaensis* at viewing distances of 1 cm (c), 3 cm (d), and 5 cm (e) using the R package "AcuityView." (f) Focal length ("f") was estimated from the centroid of the vitreous body ("c") to the distal tips of the microvillar projections ("mvp") of the photoreceptor cells, at 46 evenly spaced points around the retina (subsample shown). (g) View of a live solariellid, *I. laevissima* against aquarium substrate. Image courtesy of Dr Dai Herbert and modified from Williams et al. (2020). (h–j) View of animal in (g) at viewing distances of 1 cm (h), 3 cm (i), and 5 cm (j). Scale bars: (a) 25 μm, (f) 50 μm, and (b, g) 2.5 mm. Processed images are shown in grayscale as there is no evidence of color vision in gastropods, and to give maximum estimates of resolution.

ral substrate may be visible as estimated by AcuityView (Fig. 5h). However, these would be unclear at a distance of 3 cm and effectively invisible at 5 cm (Fig. 5i,j). Shell patterns would likely not be visible at any modeled viewing distance (Fig. 5c–e,h–j).

Discussion

SYSTEMATICS

All currently recognized solariellid genera are represented in this study and, where represented by more than one species, were recovered as clades with high support (PP = 0.99−1.00; Fig. 2). In addition, we recognize three new clades not discussed in previous studies: *Lamellitrochus* (PP = 1.00), which was included here for the first time in a molecular phylogeny; "Clade D," which includes several deep-sea species from Japan, of which two are included in this study (PP = 0.94); and a clade of species, which we initially assigned to *Bathymophila* but refer to here as "*Bathymophila*-like" that are genetically and morphologically distinct and warrant a separate genus of their own (PP = 1.00). This new genus (median minimum depth: <500 m; Fig. 3) includes all species with color patterns that were previously assigned to *Bathymophila*. Three "rogue" species are not assigned to genera or clades: "*Solariella*" *varicosa*, "*Bathymophila*" sp. 18, and "*Solariella*" *carvalhoi*. The first two are thought to belong to new genera (Williams et al. 2020) and this study suggests that a new genus may also be needed for "*Solariella*" *carvalhoi*.

This study addresses the need to include both *Lamellitrochus* and *Zetela* in a molecular phylogenetic study to determine their relationship (Williams et al. 2020). The recognition of the Atlantic genus *Lamellitrochus* as independent of *Zetela* contrasts with previous authors who synonymized the two (Marshall 1999; Williams et al. 2020). Further taxonomic work is underway to confirm species identification of remaining *Lamellitrochus* species, to name the new clades and to assign the three rogue species to new genera.

SHELL PIGMENTATION AND PATTERN

As anticipated, our data are consistent with light-dependent selection on shell pigmentation and pattern. Correlations between depth category and the presence/absence of shell pigment and pattern are apparent when these categories are divided using a range of depth cutoff values. These span almost the whole dysphotic region for pigmentation (300−900 m) and the middle range for pattern (400−700 m), with maximal support for correlations for each trait occurring around 600−700 and 400−500 m, respectively (Fig. 4b). There was support for noncorrelation in the shallow dysphotic for pigment (200 m), and at both the

shallow (200, 300 m) and deep ends of the dysphotic (800, 900 m) for pattern, indicating the presence of transition zones. Tests for correlation using depth as a continuous trait were nonsignificant, although only marginally so for pattern when tested using *brunch*. This implies that these traits are not lost continuously and evenly as depth increases from the intertidal to the abyss, but rather shell pattern is lost most rapidly in the mid-dysphotic zone, whereas pigmentation is lost most rapidly in the mid-to-deep dysphotic. The shallower transition point for pattern than pigment is expected given its dependence on pigmentation.

Losses of both shell traits occur rapidly, in line with traits subject to selection, and we found no evidence for regain, even in lineages that secondarily returned to shallower water (e.g., *Bathymophila bairdii*). Selection only acts on heritable traits, and molluscan shell pigments can be synthesized de novo, dietary in origin, or a mixture of both (Williams 2017). The red fluorescence we observed in solariellid shells is typical of porphyrin pigments, which have also been identified chemically in trochids (the same superfamily as Solariellidae) (Underwood and Creese 1976; Williams et al. 2016). Such pigmentation is stable, and its synthesis is not affected by exposure to or lack of UV light. Transcriptomic studies confirm molluscan shell porphyrins are likely synthesized de novo by trochids via the hem pathway (Williams et al. 2017), as do transcriptomic and RNAi studies in other molluscs with chemically confirmed shell porphyrins (e.g., Mao et al. 2020; Hu et al. 2021a,b). Porphyrin shell pigments are thus not derived from the snail's diet and are instead synthesized by enzymes whose presence and expression are genetically controlled. As such, this form of pigmentation, and the patterns generated by its distribution in the shell, is likely subject to selection.

Complicated, reticulated patterns with fine markings typical of shallow-water genera *Ilanga* (e.g., Fig. 1c) and *Microgaza* do not occur in genera restricted to deeper water, and pattern was recorded in only one species with a minimum depth range >700 m (*Spectamen* sp. 4). This aligns with our expectation that any selective benefits of pattern would reduce rapidly with increasing depth over a transition zone, due to limits on spatial resolution and the trade-offs between resolution and contrast sensitivity that typically occur with decreasing light availability (Tierney et al. 2017). Although the threshold we identify here (400−500 m) lies at the shallower end of the dysphotic, our findings align with calculations by Nilsson (2013, fig. 2) that high-resolution vision, needed for recognition and visual communication, becomes untenable somewhere in the range of 350−500 m. In a survey of the dysphotic zone, Johnsen (2005) found that, when present, body pigmentation was generally uniform in both pelagic and benthic species. Notable exceptions included mottling or banding of pigment on the limbs of crustaceans and spines of some sea urchins, potentially to break up the outlines of these conspicuous elongated structures.

The rarity of pigmented shells in depths >600 m aligns with many previous observations of benthic taxa in the dysphotic (e.g., Johnsen 2005), but stands in contrast to many crustaceans, fishes, and cnidarians, which tend to red, brown, or black pigmentation in increasingly deep water (Warrant and Locket 2004; Johnsen 2005). Although pigment can have nonvisual functions, such as associations with shell strength (Williams 2017), the existence of a depth threshold in pigment loss suggests that shell pigment primarily plays a visual role in solariellids. Although most of our specimens are tropical, biogeography also has an effect on distribution of shell pigment. Species occurring in cold-temperate, high-latitude waters are often colorless, even when found in shallow water (e.g., "*Solariella*" *varicosa* [Warén 1993; Høisæter 2009]).

Color vision is not known to occur in molluscs (with the exception of the firefly squid; Michinomae et al. 1994; Land and Nilsson 2012) and together with the low predicted spatial resolution of *Ilanga navakaensis* (see below), this suggests that solariellid shell color and pattern do not contribute to intraspecific recognition or communication. Instead, where there is sufficient light, shell pigmentation and pattern likely camouflage solariellids from their predators, which include fish, sea stars, and crustaceans (e.g., Pearson et al. 1984; Ventura et al. 2000; Jones 2008). In the deep sea, pigmentation can also aid crypsis by absorbing bioluminescent light; however, Johnsen (2005) proposed that pigmentation is not always necessary for crypsis of benthic taxa against the benthos in low light. The benefit of camouflage at any particular depth is affected by the number of visual predators and the role vision plays in predator foraging. Unlike gastropods, many fish and crustaceans have high-resolution vision and some can distinguish colors (Marshall 2017). Studies of intertidal molluscs show that shell color and pattern can play important roles in camouflage from such predators (e.g., Smith 1975; Shigemiya 2004), but deep-sea predators, such as king crabs and macrourid fish that feed on solariellids in the dysphotic and aphotic zones (Pearson et al. 1984; Jones 2008), may rely more on chemosensory cues (Kotrschal et al. 1998). A shift with increased depth from visual predator species to chemosensory predators would further decrease the evolutionary benefits of pigmentation and pattern in the deep sea and may explain the pronounced thresholds for pattern and pigmentation. Furthermore, surveys show that Caribbean molluscivorous fish and crabs are rare below 500 m (Walker et al. 2002) and other ecological studies show that predator diversity is lowest on the abyssal plain (Harper and Peck 2016).

EYE FUNCTION

As in shell traits, we found strong support for noncorrelation between depth and "vision" when depth categories were divided at the shallow or deep extremes of the dysphotic zone, with

support decreasing from both ends approaching a transition point at 500 m. Here, we found very weak support for the dependent model (correlation with depth category). This suggests that 500 m could be a transition point for "vision"; that is, although eyes may be advantageous in shallow-water species, they are likely of limited use below 500 m. We also found a marginally nonsignificant correlation between loss of "vision" and depth using *threshBayes* with continuous depth data. Weak correlations of loss of "vision" with depth using both binarized and continuous depth data suggest that there may be a more gradual loss with depth than occurs with shell pigment and pattern, counter to our expectations.

Solariellids are unlikely to use vision for tasks requiring high resolution such as object recognition, ruling out the possibility that shell pigmentation and pattern are used for intraspecific communication (Fig. 5c-e,h-j). Their eyes lack a cornea and lens, with only the vitreous body providing any kind of optical function (Sasaki 1998; Sumner-Rooney et al. 2016). We estimated an interreceptor angle of 4.3° in the shallow-water species *Ilanga navakaensis*, which would place it at the lower boundary of "high-resolution vision" if it reflected visual acuity (Nilsson 2013). However, the likely poor focusing power of the vitreous body means that the interreceptor angle is unlikely to be the limiting factor, and acuity may therefore be substantially poorer than 4.3°. Furthermore, the calculated optical sensitivity of *I. navakaensis* in shallow water (0.5) is an order of magnitude lower than both octopus (9.7) and *Pecten* (4.0), which also inhabit coastal benthic habitats (Land and Nilsson 2012). It is therefore likely that visual performance is poor, even in well-lit, shallow water. In deep water, *I. navakaensis*'s estimated sensitivity (1.0) compares extremely poorly to deep-sea fish and crustaceans, which boast sensitivities in the order of the hundreds or thousands (Land and Nilsson 2012).

Animals with low-resolution eyes like solariellids may use them for predator detection (usually the detection of shadows or moving objects), habitat selection, or orientation to static objects (Nilsson 2013). Solariellids are capable of rapidly burrowing into sediment or swimming short distances. Some South African species of *Ilanga*, *Spectamen*, and *Solariella* have been observed to swim up to 30 cm by rapidly moving the foot side to side, and this is presumed to be an escape response to predators (Herbert 1987). Nilsson (2013) estimated that low-resolution vision would generally be useful only to depths of around 300 m in clear water in the absence of bioluminescence. Although we detected a deeper transition zone, this discrepancy could reflect several factors, including the weak nature of the relationship or the possible position of solariellid vision on the boundary of "low" and "high" resolution. Alternatively, deep-water solariellids may use their eyes to detect bioluminescent light, associated either directly or indirectly, with predators (e.g., macrourid fish, which have bioluminescent light organs [Dunlap et al. 2013]). Syme and Oakley (2012) and Juarez et al. (2019) found significant relationships between depth and lateral eye loss in cylindroleberid ostracods using thresholds of 1,000 m, beyond the penetration of sunlight. This suggests a deeper transitional zone in ostracods, which may also result from a greater relevance of bioluminescence or role of vision, but highlights the context-dependent nature of loss, both phylogenetically and ecologically (Dunlap et al. 2013).

The lack of a stronger correlation between "vision" and depth is surprising at first, but there are only a minimum of seven independent losses of "vision" across the phylogeny (vs. a minimum of 15 for pigmentation and 16 for pattern) making the tests statistically weaker. Additionally, as our assessment is based on gross external morphology only, animals may be effectively blind before we record them as such. Our data for "vision," therefore, are conservative, and sight may be lost more frequently, and at shallower depths, than recorded here. Phylogenetic uncertainty for relationships among genera also contributes to the weak correlations seen in BAYESTRAITS, because several losses are at the generic level. Tests for phylogenetic signal, however, suggest that the distribution of pigmentation, pattern, and "vision" is nonrandom across the solariellid phylogeny, with "vision" more "clumped" than might be expected. In fact, many of the blind species are found in just two genera: *Phragmomphalina* and *Bathymophila*. Depth also shows a strong phylogenetic signal, so phylogenetic signal in any of the morphological traits also mirrors (to some extent) depth.

EVOLUTION OF TRAIT LOSS

Shell pigment, pattern, and "vision" presumably confer selective advantages to solariellids living in shallower waters; however, this advantage likely decreases as depth increases. The fact that trait loss has evolved a different number of times (more often for shell traits than "vision"), at different speeds (faster for shell traits than "vision"), and across a larger time range for shell traits (Paleocene-Pliocene) than "vision" (Early Eocene-Late Miocene) suggests that there are differences in the strength or nature of selection pressures acting on each trait. Visual processes are energetically expensive, and morphologically and neurologically complex (Niven and Laughlin 2008). Similarly, the production, modification, and deposition of shell pigments are also likely to be metabolically costly (Williams 2017). The pathways involved in pigment production and deposition are not fully known, and may vary between taxa, but we suggest they are likely to be less complex than the development and maintenance of eyes.

The precise mechanisms underlying trait losses in solariellids remain uncertain. Transcriptomic, quantitative genetic, and breeding studies would help to determine whether trait loss is due to a single mutation or the accumulation of multiple deleterious mutations, to identify the role of pleiotropy, and whether modifications affect one or more genetic pathways (e.g., Protas et al.

2011). Breeding studies are not possible for solariellids, which are rare and difficult to collect, but transcriptomics of selected taxa could provide some insight in future studies.

Conclusions

The large number of molluscan families that span the ocean depths provide a plethora of opportunities for studying parallel and convergent evolution of pigmentation and eye loss in the deep sea. Moreover, the myriad diversity of eye morphologies of Mollusca offers exciting opportunities for comparison among highly divergent evolutionary visual systems. Here, we demonstrate for the first time that evolutionary losses of eye function in simple pit eyes, shell pigmentation, and shell color pattern are explicitly associated with deep-water habitats in solariellid snails. We show that loss of all three traits occurs rapidly within the dysphotic region, with maximum support for correlation for loss of pigmentation at greater depth than observed for loss of shell pattern or eyes, although eyes can be found in deeper specimens than shell traits. Estimates of poor visual acuity and the order of trait loss suggest that shell color and pattern are not used for communication with conspecifics. Instead, they may provide camouflage from visual predators that are less common (or rely less on vision) in the deeper part of the dysphotic zone. We show here that selection pressures and phylogeny likely play a role in the evolution of trait loss in solariellids. Although not tested, selection for the three traits examined here may follow different pathways in different species (Sumner-Rooney et al. 2016). Future studies could investigate whether the pathways of trait loss differ in different solariellids by using transcriptomics to determine how visual and pigmentation pathways compare across species.

AUTHOR CONTRIBUTIONS

STW conceived the original idea, provided resources, wrote the first draft, supervised ESN, and acquired funding. STW and LSR edited the text and made figures. ESN, LMS, LSR, and STW collected data.

ACKNOWLEDGMENTS

We thank Y. Kano (University of Tokyo), B. Marshall (Museum of New Zealand Te Papa Tongarewa), and D. Herbert (previously KwaZulu-Natal Museum) for the loan of specimens and for advice on species traits; J. Serb and an anonymous reviewer for constructive comments on an earlier version of the manuscript; D. Herbert for providing the image of *Ilanga laevissima*; C. Whisson and L. Kirkendale (Western Australian Museum) for the loan of specimens; D. Cavallari for advice on traits for "*Solariella*" *carvalhoi*; A. Salvador for registering NHMUK specimens; P. Foster for scripts used to clean up datasets; and N. Cooper for advice with R. We also particularly thank P. Bouchet, B. Buge, N. Puillandre, and V. Héros for arranging the loan of numerous Muséum national d'histoire naturelle (MNHN) samples, without which this study would not have been possible. MNHN material was collected during expeditions of the "Tropical Deep-Sea Benthos" program under PIs Richer de Forges, Bouchet, Samadi, Chen: BIOPAPUA, BOA1, BORDAU1, CONCALIS, EBISCO, EXBODI, KARUBENTHOS2, KAVIENG2014, MAINBAZA, MIRIKY, NANHAI2014, NORFOLK2, PANGLAO2005, PAPUANIUGUINI, SALOMON2, SANTO2006, TARASOC, TERRASSES, and ZHONGSHA2015. The PIs acknowledge the Flotte Océanographique Française, Institut de Recherche pour le Développement, the Philippines Bureau of Fisheries and Aquatic Resources, and National Taiwan Ocean University for ship time, and the Total Foundation and Prince Albert II of Monaco Foundation for additional support. For material collected during PANGLAO2004, SANTO2006, and KARUBENTHOS expeditions, Bouchet also acknowledges the support of the Stavros Niarchos Foundation, Lounsbery Foundation, and Parc National de la Guadeloupe. For the context of the expeditions, see Bouchet et al. (2008) and http://expeditions.mnhn.fr/?lang=en_US. This work was supported by Departmental Investment Funding from The Natural History Museum, London to STW.

CONFLICT OF INTEREST

The authors declare no conflict of interest.

DATA ARCHIVING

All data are available from online databases (GenBank http://www.ncbi.nlm.nih.gov/nucleotide/) or the Supporting Information.

LITERATURE CITED

Abouheif, E. (1999) A method for testing the assumption of phylogenetic independence in comparative data. *Evolutionary Ecology Research*, 1, 895–909.

Bagirov, N.E. (1995) Four new species of deep-water molluscs of the subfamily Solariellinae (Gastropoda: Trochidae) from the North-Western Pacific. *Ruthenica*, 5, 1–7.

Beu, A.G. (1990) Cenozoic Mollusca of New Zealand. *New Zealand Geological Survey paleontological bulletin*, 58, 1–518.

Bielejec, F., Rambaut, A., Suchard, M.A. & Lemey, P. (2011) SPREAD: spatial phylogenetic reconstruction of evolutionary dynamics. *Bioinformatics*, 27, 2910–2912.

Blomberg, S.P., Garland, T. Jr. & Ives, A.R. (2003) Testing for phylogenetic signal in comparative data: behavioral traits are more labile. *Evolution*, 57, 717–745.

Bouchet, P., Héros, V., Lozouet, P. & Maestrati, P. (2008) A quarter-century of deep-sea malacological exploration in the South and West Pacific: where do we stand? How far to go. *Tropical deep-sea Benthos*, 25, 9-40.

Castresana, J. (2000) Selection of conserved blocks from multiple alignments for their use in phylogenetic analysis. *Molecular Biology and Evolution*, 17, 540–552.

Caves, E.M. & Johnsen, S. (2017) AcuityView: an R package for portraying the effects of visual acuity on scenes observed by an animal. *Methods in Ecology and Evolution*, 9, 793-797.

Darriba, D., Posada, D., Kozlov, A.M., Stamatakis, A., Morel, B. & Flouri, T. (2020) ModelTest-NG: a new and scalable tool for the selection of DNA and protein evolutionary models. *Molecular Biology and Evolution*, 37, 291-294.

Drummond, A.J. & Rambaut, A. (2007) BEAST: Bayesian evolutionary analysis by sampling trees. *BMC Evolutionary Biology*, 7, 214.

Dunlap, P.V., Takami, M., Wakatsuki, S., Hendry, T.A., Sezaki, K. & Fukui, A. (2013) Inception of bioluminescent symbiosis in early developmental stages of the deep-sea fish, *Coelorinchus kishinouyei* (Gadiformes: Macrouridae). *Ichthyological Research*, 61, 59-67.

Fritz, S.A. & Purvis, A. (2010) Selectivity in mammalian extinction risk and threat types: a new measure of phylogenetic signal strength in binary traits. *Conservation Biology*, 24, 1042-1051.

Gilks, W.R. (1996) Introducing Markov chain Monte Carlo. Markov chain Monte Carlo in practice. Chapman and Hall, Lond.

Gill, M.S., Tung Ho, L.S., Baele, G., Lemey, P. & Suchard, M.A. (2017) A relaxed directional random walk model for phylogenetic trait evolution. *Systematic Biology*, 66, 299-319.

Gonzalez, B.C., Worsaae, K., Fontaneto, D. & Martínez, A. (2017) Anophthalmia and elongation of body appendages in cave scale worms (Annelida: Aphroditiformia). *Zoologica Scripta*, 47, 106-121.

Harper, E.M. & Peck, L.S. (2016) Latitudinal and depth gradients in marine predation pressure. *Global Ecology and Biogeography*, 25, 670-678.

Herbert, D.G. (1987) Revision of the Solariellinae (Mollusca: Prosobranchia: Trochidae) in southern Africa. *Annals of the Natal Museum*, 28, 283-382.

Høisæter, T. (2009) Distribution of marine, benthic, shell bearing gastropods along the Norwegian coast. *Fauna norvegica*, 28, 5-106.

Hu, B., Li, Q. & Yu, H. (2021a) RNA interference by ingested dsRNA-expressing bacteria to study porphyrin pigmentation in *Crassostrea gigas*. *International journal of molecular sciences*, 22, 6120.

Hu, B., Li, Q., Yu, H. & Du, S. (2021b) Identification and characterization of key haem pathway genes associated with the synthesis of porphyrin in Pacific oyster (*Crassostrea gigas*). *Comparative Biochemistry and Physiology Part B: Biochemistry and Molecular Biology*, 255, 110 595.

Johnsen, S. (2005) The red and the black: bioluminescence and the color of animals in the deep sea. *Integrative and Comparative Biology*, 45, 234-246.

Jones, M.R.L. (2008) Dietary analysis of *Coryphaenoides serrulatus*, *C. subserruiatus* and several other species of macrourid fish (Pisces: Macrouridae) from northeastern Chatham Rise, New Zealand. *New Zealand Journal of Marine and Freshwater Research*, 42, 73-84.

Juarez, B.H., Speiser, D.I. & Oakley, T.H. (2019) Context-dependent evolution of ostracod morphology along the ecogeographical gradient of ocean depth. *Evolution; international journal of organic evolution*, 73, 1213-1225.

Katoh, K., Asimenos, G. & Toh, H. (2009) Multiple alignment of DNA sequences with MAFFT. Pp. 39–64 *in* Posada, D., ed. Bioinformatics for DNA sequence analysis. Springer, Berlin.

Keck, F., Rimet, F., Bouchez, A. & Franc, A. (2016) *phylosignal*: an R package to measure, test, and explore the phylogenetic signal. *Ecology and evolution*, 6, 2774-2780.

Kiel, S. (2010) On the potential generality of depth-related ecologic structure in cold-seep communities: evidence from Cenozoic and Mesozoic examples. *Palaeogeography, Palaeoclimatology, Palaeoecology*, 295, 245-257.

Kiel, S. & Bandel, K. (2001) Trochidae (Archaeogastropoda) from the Campanian of Torallola in northern Spain. *Acta Geologica Polonica*, 51, 137-154.

Kiel, S., Bandel, K. & de CPerrilliat, M. (2002) New gastropods from the Maastrichtian of the Mexcala Formation in Guerrero, southern Mexico, part II: Archaeogastropoda, Neritimorpha and Heterostropha.(With 3 figures). *Neues Jahrbuch für Geologie und Paläontologie Abhandlungen*, 226, 319-342.

Kotrschal, K., Van Staaden, M. & Huber, R. (1998) Fish brains: evolution and anvironmental relationships. *Reviews in Fish Biology and Fisheries*, 8, 373-408.

Land, M.F. (1981) Optics and vision in invertebrates. Pp. 471–592. *in* Autrum, H., ed. Handbook of sensory physiology. Volume VII/6B. Vision in invertebrates: A: invertebrate photoreceptors. Springer, Berlin.

Land, M.F. & Nilsson, D.-E. (2012) Animal eyes. Oxford Univ. Press, Oxford, U.K.

Lemey, P., Suchard, M. & Rambaut, A. (2009) Reconstructing the initial global spread of a human influenza pandemic: a Bayesian spatial-temporal model for the global spread of H1N1pdm. *PLOS Currents*, 1, RRN1031.

Mao, J., Zhang, Q., Yuan, C., Zhang, W., Hu, L., Wang, X., Liu, M., Han, B., Ding, J. & Chang, Y. (2020) Genome-wide identification, characterisation and expression analysis of the ALAS gene in the Yesso scallop (*Patinopecten yessoensis*) with different shell colours. *Gene*, 757, 144925.

Marshall, B.A. (1999) A revision of the Recent Solariellinae (Gastropoda: Trochoidea) of the New Zealand region *The Nautilus*, 113, 4-42.

Marshall, J. (2017) Vision and lack of vision in the ocean. *Current Biology*, 27, R494-R502.

Michinomae, M., Masuda, H., Seidou, M. & Kito, Y. (1994) Structural basis for wavelength discrimination in the banked retina of the firefly squid *Watasenia scintillans*. *The Journal of Experimental Biology*, 193, 1–12.

Minin, V.N., Bloomquist, E.W. & Suchard, M.A. (2008) Smooth skyride through a rough skyline: Bayesian coalescent-based inference of population dynamics. *Molecular Biology and Evolution*, 25, 1459-1471.

Mirarab, S., Nguyen, N. & Warnow, T. (2014) PASTA: ultra-large multiple sequence alignment. Pp. 177–191 in Sharan, R., ed. Research in computational molecular biology. Springer, Cham, Switzerland.

Moran, P.A. (1948) The interpretation of statistical maps. *Journal of the Royal Statistical Society. Series B (Methodological)*, 10, 243-251.

Moran, P.A. (1950) Notes on continuous stochastic phenomena. *Biometrika*, 37, 17-23.

Munk, O. (1965) Ocular degeneration in deep-sea fishes. *Galathea-Rep*, 8, 21-31.

Münkemüller, T., Lavergne, S., Bzeznik, B., Dray, S., Jombart, T., Schiffers, K. & Thuiller, W. (2012) How to measure and test phylogenetic signal. *Methods in Ecology and Evolution*, 3, 743-756.

Nilsson, D.E. (2013) Eye evolution and its functional basis. *Visual Neuroscience*, 30, 5-20.

Niven, J.E. & Laughlin, S.B. (2008) Energy limitation as a selective pressure on the evolution of sensory systems. *The Journal of Experimental Biology*, 211, 1792-1804.

Orme, D., Freckleton, R., Thomas, G., Petzoldt, T., Fritz, S., Isaac, N. & Pearse, W. (2012) Caper: comparative analyses of phylogenetics and evolution in R. R package version 0.5.2, 458.

Orme, D., Freckleton, R., Thomas, G., Petzoldt, T., Fritz, S., Isaac, N. & Pearse, W. (2013) The caper package: comparative analysis of phylogenetics and evolution in R. R package version 5, 1-36.

Pagel, M. (1999) Inferring the historical patterns of biological evolution. *Nature*, 401, 877-884.

Pagel, M. & Meade, A. (2007) BayesTraits. Available via http://www.evolution.rdg.ac.uk/BayesTraits.html.

Pearson, W., Woodruff, D. & Higgins, B. (1984) Feeding ecology of juvenile king and Tanner crab in the southeastern Bering Sea. Final Report, Outer Continental Shelf Environmental Assessment Program. Battell Pacific Northwest Lab, Richland, WA.

Plummer, M., Best, N., Cowles, K. & Vines, K. (2006) CODA: convergence diagnosis and output analysis for MCMC. *R news*, 6, 7-11.

Price, M.N., Dehal, P.S. & Arkin, A.P. (2009) FastTree: computing large minimum evolution trees with profiles instead of a distance matrix. *Molecular Biology and Evolution*, 26, 1641–1650.

Protas, M.E., Trontelj, P. & Patel, N.H. (2011) Genetic basis of eye and pigment loss in the cave crustacean, *Asellus aquaticus*. *Proceedings of the National Academy of Sciences*, 108, 5702-5707.

Purvis, A. & Rambaut, A. (1995) Comparative analysis by independent contrasts (CAIC): an Apple Macintosh application for analysing comparative data. *Bioinformatics (Oxford, England)*, 11, 247-251.

Quinn, J.F., Jr. (1979) Biological results of the University of Miami deep-sea expeditions. 130. The systematics and zoogeography of the gastropod family Trochidae collected in the Straits of Florida and its approaches. *Malacologia*, 19, 1-62.

Rambaut, A., Drummond, A.J., Xie, D., Baele, G. & Suchard, M.A. (2018) Posterior summarization in Bayesian phylogenetics using Tracer 1.7. *Systematic biology*, 67, 901–904.

Revell, L.J. (2012) phytools: an R package for phylogenetic comparative biology (and other things). *Methods in ecology and evolution*, 3, 217-223.

Sasaki, T. (1998) Comparative anatomy and phylogeny of the recent Archaeogastropoda (Mollusca: Gastropoda). *Univ. Tokyo Bull*, 38, 1-223.

Shigemiya, Y. (2004) Reversible frequency-dependent predation of a puffer, Takifugu niphobles (Pisces: Tetraodontidae), related to spatial distribution of colour-polymorphic prey. *Biological Journal of the Linnean Society*, 81, 197-202.

Smith, D. (1975) Polymorphism and selective predation in *Donax faba* Gmelin (Bivalvia: Tellinacea). *Journal of Experimental Marine Biology and Ecology*, 17, 205-219.

Sumner-Rooney, L. (2018) The kingdom of the blind: disentangling fundamental drivers in the evolution of eye loss. *Integrative and Comparative Biology*, 58, 372-385.

Sumner-Rooney, L., Kenny, N.J., Ahmed, F. & Williams, S.T. (2019) The utility of micro-computed tomography for the non-destructive study of eye microstructure in snails. *Scientific Reports*, 9, 15411.

Sumner-Rooney, L., Sigwart, J.D., McAfee, J., Smith, L. & Williams, S.T. (2016) Repeated eye reduction events reveal multiple pathways to degeneration in a family of marine snails. *Evolution; international journal of organic evolution*, 70, 2268-2295.

Syme, A.E. & Oakley, T.H. (2012) Dispersal between shallow and abyssal seas and evolutionary loss and regain of compound eyes in cylindroleberidid ostracods: conflicting conclusions from different comparative methods. *Systematic Biology*, 61, 314-336.

Tierney, S.M., Friedrich, M., Humphreys, W.F., Jones, T.M., Warrant, E.J. & Wcislo, W.T. (2017) Consequences of evolutionary transitions in changing photic environments. *Austral Entomology*, 56, 23-46.

Underwood, A.J. & Creese, R.G. (1976) Observations on the biology of the trochid gastropod *Austrocochlea constricta* (Lamarck) (Prosobranchia). II. The effects of available food on shell-banding pattern. *Journal of Experimental Marine Biology and Ecology*, 23, 229-240.

Ventura, C., Grillo, M. & Fernandes, F. (2000) Feeding niche breadth and feeding niche overlap of paxillosid starfishes (Echinodermata: Asteroidea) from a midshelf upwelling region, Cabo Frio, Brazil. Pp. 227–233. *in* Barker, M., ed. Echinoderms. Swets & Zeitlinger, Lisse, The Netherlands.

Vilvens, C. & Williams, S.T. (2020) New species of *Ilanga* (Gastropoda: Trochoidea: Solariellidae) from the Indo-West Pacific. *Zootaxa*, 4732, 201–257.

Vilvens, C., Williams, S.T. & Herbert, D.G. (2014) New genus *Arxellia* with new species of Solariellidae (Gastropoda: Trochoidea) from New Caledonia, Papua New Guinea, Philippines, Western Australia, Vanuatu and Tonga. *Zootaxa*, 3826, 255-281.

Walker, S.E., Parsons-Hubbard, K., Powell, E. & Brett, C.E. (2002) Predation on experimentally deployed molluscan shells from shelf to slope depths in a tropical carbonate environment. *Palaios*, 17, 147-170.

Warén, A. (1993) New and little known Mollusca from Iceland and Scandinavia. Part 2. *Sarsia*, 78, 159-201.

Warrant, E.J. & Locket, N.A. (2004) Vision in the deep sea. *Biological Reviews*, 79, 671-712.

Warrant, E.J. & Nilsson, D.-E. (1998) Absorption of white light in photoreceptors. *Vision research*, 38, 195-207.

Wheeler, T.J. & Kececioglu, J.D. (2007) Multiple alignment by aligning alignments. *Bioinformatics*, 23, i559–i568.

Williams, S.T. (2017) Molluscan shell colour. *Biological reviews of the Cambridge Philosophical Society*, 92, 1039-1058.

Williams, S.T., Ito, S., Wakamatsu, K., Goral, T., Edwards, N.P., Wogelius, R.A., Henkel, T., de Oliveira, L.F., Maia, L.F., Strekopytov, S., et al. (2016) Identification of shell colour pigments in marine snails *Clanculus pharaonius* and *C. margaritarius* (Trochoidea; Gastropoda). *PloS one*, 11, e0156664.

Williams, S.T., Kano, Y., Warén, A. & Herbert, D.G. (2020) Marrying molecules and morphology: first steps towards a reevaluation of solariellid genera (Gastropoda: Trochoidea) in the light of molecular phylogenetic studies. *Journal of Molluscan Studies*, 86, 1-26.

Williams, S.T., Karube, S. & Ozawa, T. (2008) Molecular systematics of Vetigastropoda: Trochidae, Turbinidae and Trochoidea redefined. *Zoologica Scripta*, 37, 483-506.

Williams, S.T., Lockyer, A.E., Dyal, P., Nakano, T., Churchill, C.K.C. & Speiser, D.I. (2017) Colorful seashells: identification of haem pathway genes associated with the synthesis of porphyrin shell color in marine snails. *Ecology and evolution*, 7, 10379-10397.

Williams, S.T. & Ozawa, T. (2006) Molecular phylogeny suggests polyphyly of both the turban shells (family Turbinidae) and the superfamily Trochoidea (Mollusca: Vetigastropoda). *Molecular Phylogenetics and Evolution*, 39, 33-51.

Williams, S.T., Smith, L.M., Herbert, D.G., Marshall, B.A., Warén, A., Kiel, S., Dyal, P., Linse, K., Vilvens, C. & Kano, Y. (2013) Cenozoic climate change and diversification on the continental shelf and slope: evolution of gastropod diversity in the family Solariellidae (Trochoidea). *Ecology and evolution*, 3, 887-917.

Associate Editor: J. Day
Handling Editor: A. G. McAdam

Supporting Information

Additional supporting information may be found online in the Supporting Information section at the end of the article.

Table S1. Table listing species, sampling details and GenBank Accession Numbers for all specimens included in Figure 2. Specimens with new sequence data are in bold (OK392049– OK392072; OK393746–OK393767; OK393769– OK393793; OK393794–OK393817).

Table S2. Morphological trait data. Species with new eye data are in bold font; where different, name used in Williams et al. (2013), Sumner-Rooney et al. (2016) or Williams et al. (2020) is given in parentheses. Pigmentation and pattern data are new to this study. Notes on depth indicate whether data came from molecular specimens only, with the reason in parentheses (species ID: only known from molecular samples; species delimitation: molecular results indicate that there is some confusion about species boundaries), or literature reports (references given).

Table S3. List of species examined under UV light.

Table S4 (in separate file). Fasta file of four gene alignment. Note that alignment excludes bases removed by Gblocks.

Table S5. Mean rate of change and 95% highest posterior density intervals (HPD) between character states for shell pigmentation, shell pattern and 'vision' in solariellid snails using an asymmetric, non-BSSVS substitution model, as implemented in BEAST and read in TRACER.

Table S6. Testing for correlation between morphological traits (pigmentation, pattern, 'vision') and depth. Depth bin and Log Marginal Likelihood (average of three runs) and Bayes Factor for each trait testing 500 BEAST trees.

Figure S1. Local Moran's I (I_i) values for log transformed depth data, random data and Brownian model plotted onto the phylogenetic tree from Figure 2.